RSC Advances

This article can be cited before page numbers have been issued, to do this please use: H. Huang, X. Zhang, X. Jiang, K. Dou, Z. NI and H. Lu, *RSC Adv.*, 2016, DOI: 10.1039/C6RA06400K.

ROYAL SOCIETY OF CHEMISTRY

www.rsc.org/advances

View Article Online
DOI: 10.1039/C6RA06400K

RSC Advances

COMMUNICATION

Hollow anatase TiO_2 nanoparticles with excellent catalytic activity for dichloromethane combustion

Received 00th 00000 2016,
Accepted 00th 00000 20xx

DOI: 10.1039/x0xx00000x

www.rsc.org/

Haifeng Huang,[a] Xixiong Zhang,[a] Xiaojia Jiang,[a] kang Dou,[a] Zhiyi Ni [a] and Hanfeng Lu *[b]

Toward the design of efficient nanocatalysts, hollow anatase TiO_2 nanoparticles with around 11.4 nm were prepared by cetyltrimethylammonium bromide (CTAB) -assisted hydrothermal method. This catalyst delivered a high catalytic activity for dichloromethane (DCM) combustion, in particular, the catalyst exhibited 90% DCM conversion at 201 °C. The satisfactory performance of the catalyst can be contributed to the hollow texture with rich active sites and the high amount of moderately strong acidic sites on the hollow TiO_2 surface.

Chlorinated volatile organic compounds (CVOCs) are poisonous pollutants considered as the most harmful organic contaminants because of their acute toxicity and strong bioaccumulation potential. Abatement of alkyl chloride pollutants, such as dichloromethane (DCM), 1, 2-dichloroethane (DCE) and trichloroethylene (TCE), has gained considerable attention because of increasing concern for environmental protection.[1] Among various available detoxification techniques, catalytic oxidation is a promising method to abate these harmful emissions due to its low energy consumption, high efficiency, and preferred ability of converting CVOCs into harmless substances.[2-4] Catalyst is undoubtedly a key factor controlling this technique [5]. Nowadays, the most frequently investigated catalysts for CVOCs removal include three typeset of catalysts based on noble metals [6-9], transition metal oxides [10-15], or zeolites [16]. The catalytic oxidation of DCM, a representative alkyl chloride pollutant, has been widely investigated on these catalysts.[17-19] Noble metal catalysts, such as Pt catalysts and Ru catalysts are more preferentially acceptable than other catalysts. However, expensive price and shortage of resources limit its industrial application.[1,20] Therefore, developing an ideal catalyst that is earth-abundant, contains non-noble metals, and possesses superior catalytic activity will be a breakthrough in DCM catalytic combustion. DCM can readily react with the hydroxyl groups of catalysts to form reactive intermediates, which can be oxidized to carbon dioxide.[17,18] It is believed that the activity for catalytic combustion of DCM is usually determined by several key factors such as surface acidity and redox properties.[21, 22] The strength and the amount of medium and strong acidic sites would be beneficial for the chemisorption of DCM molecules onto the hydroxyl groups of the catalyst surface.[5, 23] Metal oxide catalysts with strong acidic surface show a very high catalytic activity in the combustion of CVOCs,[24-25] however, coke formation readily occurs on catalysts, leading to bad stability and restricting their development.[26] Therefore, it is meaningful to adjust the structure of metal oxide materials, such as Al_2O_3, SiO_2, and TiO_2, to ensure the high catalytic activity and stability for CVOC combustion, especially for TiO_2 who is more resistant to acidic species among metal oxides.[27-29] TiO_2 have various crystal structures, which can be readily controlled. Different TiO_2 crystal structures may exhibit different catalytic activities; thus, regulating and controlling the crystal structures may help us find an optimum catalyst. Herein, we reported a hollow anatase TiO_2 (TiO_2-HA) nanoparticle catalyst prepared by CTAB-assisted hydrothermal synthesis. As reference, we also prepared brookite TiO_2 (TiO_2-B), rutile TiO_2 (TiO_2-R), and six other TiO_2 catalysts. The TiO_2-HA nanoparticle catalyst shows the highest activity among all the employed catalysts, including noble metal catalysts reported in other papers.[7,17,20] The structure and surface chemical properties of the TiO_2-HA were characterized, and the catalytic behavior was assessed in relation to a few important parameters of the catalysts such as surface acidity and reducibility. We expect that findings presented in this paper could provide novel insights into the design and synthesis of catalysts for catalytic oxidation of CVOCs.

Hollow anatase nanoparticles were synthesized through CTAB-assisted hydrothermal method. Specific amounts of precursors, namely, $TiOSO_4 \cdot 2H_2O$ and CTAB (CTAB/$TiOSO_4$ = 1:12, molar ratio) were dissolved in 50 mL of deionized water under magnetic stirring at 60 °C. The $TiOSO_4$ solution was added to the CTAB solution under vigorous stirring. The liquid mixture obtained was then subjected to hydrothermal treatment in a 150 mL stainless steel autoclave at 110 °C for 24 h. After the autoclave was cooled to room temperature, the precipitate was filtered and washed repeatedly with deionized water and ethyl alcohol. TiO_2-B and TiO_2-R were synthesized through modified hydrothermal method by using previously described method.[30, 31] The detailed synthesis of other catalysts was introduced in the

[a] College of Environment, ZheJiang University of Technology, Hangzhou 310014, PR China.
[b] College of Chemical Engineering, ZheJiang University of Technology, Hangzhou 310014, PR China. E-mail: luhf@zjut.edu.cn; Tel: +86-571-88320767.
Electronic Supplementary Information (ESI) available: [details of any supplementary information available should be included here]. See DOI: 10.1039/x0xx00000x

View Article Online
DOI: 10.1039/C6RA06400K

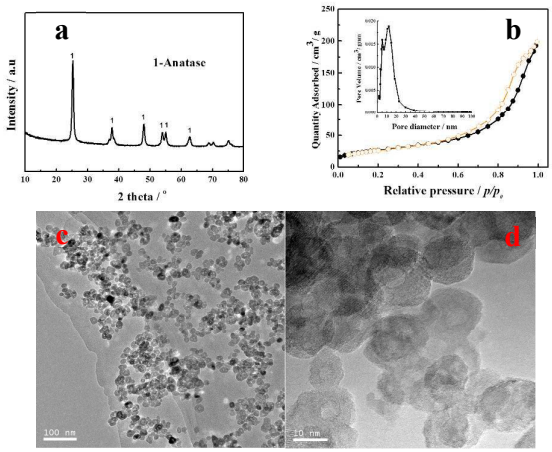

Fig. 1 Characterizations of hollow anatase TiO_2 (TiO_2-HA). (a) the XRD pattern of TiO_2-HA; (b) N_2 adsorption-desorption curves and pore size distribution of TiO_2-HA; (c, d) HRTEM images of TiO_2-HA.

supporting material. Almost all precursors prepared were calcined in air at 500 °C for 4 h. The catalysts were characterized by sensitive physico-chemical techniques, such as X-ray diffraction (XRD), N_2-physisorption, transmission electron microscopy (TEM), and pyridine adsorption followed by FT-IR spectroscopy (FTIR-pyridine) analyses.

Catalytic performance tests were performed in a traditional fixed-bed tubular reactor (quartz glass; 6 mm i.d.) at ambient pressure. Briefly, 200 mg of the catalyst was placed in the middle of the reactor and diluted with 1800 mg of quartz sand. DCM feed gas was generated by bubbling air (20.8% O_2 and 79.2% N_2) at a suitable flow rate through a saturator in an ice bath. A bypass flow of air was also used to balance total flow rate to provide the desired gas hourly space velocity (GHSV) in the catalyst bed. The gas stream was composed of 1000 ppm DCM and air in 50 mL min^{-1} [GHSV of 15000 mL h^{-1} $(gcat.)^{-1}$]. The effluent gases were analyzed online with a GC-6890N gas chromatograph equipped with FID detector and an FT-IR spectrometer (Vertex70; scan rate = 32 scans s^{-1}; resolution = 2.5 cm^{-1}). GC–MS analysis was conducted to confirm the formation of by-products. The concentrations of Cl_2 and HCl were analyzed by bubbling the effluent through 0.0125 N NaOH solution. Further detailed analytic process was described in a previous study.[32]

Fig.1a presents the XRD pattern of the TiO_2-HA catalyst. The sample shows characteristic diffraction peaks of the anatase TiO_2 crystalline phase (PDF#21-1272) and no other diffraction peaks were detected, also TiO_2-B and TiO_2-R catalysts respective show the characteristic diffraction peaks of the brookite and rutile TiO_2 crystalline phase (see Fig.S1). The texture properties of various catalysts were investigated by N_2 adsorption / desorption. As shown in Table 1, the TiO_2-HA catalyst exhibits higher BET specific surface area than the two other catalysts. The N_2 adsorption / desorption isotherms and the BJH pore size distribution of the TiO_2-HA catalyst are shown in Fig.1b. The sample exhibits type IV adsorption / desorption isotherms with H1 hysteresis loops, which are typical characteristics of mesoporous materials according to the IUPAC classification.[33, 34]As shown in the inset of Fig.1b, the catalyst possesses a symmetrical mesoporous distribution within 5-25 nm. Moreover, the pore volume of TiO_2-HA is larger than that of TiO_2-B or TiO_2-R, which can promote the

Table 1 The textures and catalytic performances of TiO_2 catalysts

catalysts	BET surface area (m^2/g)	Pore volume (cm^3/g)	Pore size(nm)	Particle size(Å)	T_{50} /°C	T_{90} /°C
TiO_2-HA	94.73	0.31	12.98	114	175	201
TiO_2-B	36.08	0.27	29.95	338	241	279
TiO_2-R	19.51	0.26	52.68	390	302	411

adsorption and activation of DCM molecules on the internal surface of the catalysts. To investigate the morphology and dispersion of the samples, the representative TEM patterns of the catalysts were obtained (TiO_2-HA see Fig.1c-d, TiO_2-B, TiO_2-R see Fig.S2). It can be seen that the particles of TiO_2-HA show good dispersion, and the nanoparticles show regular homogeneous particles with hollow spherical morphology. HRTEM confirms the existence of 8-20 nm TiO_2 particles. This findings is in good agreement with the average mean diameter estimated according to the Scherrer equation applied to the<101> reflection of anatase of the XRD data (see Table 1). The hollow pore size of the particle corresponds to the mesoporous distribution shown in Fig.1b (inset). Hence, TiO_2-HA nanoparticle is a catalyst that belongs to anatase crystalline phase and possesses hollow spherical morphology. Higher specific surface area, wider pore-size distribution of mesoporous, larger pore volume and hollow spherical morphology may be favorable for the improvement of the catalytic performance for DCM destruction.

The catalytic activity of the TiO_2 catalysts for DCM decomposition is shown in fig.2a. The TiO_2-HA and TiO_2-B catalysts present a high catalytic activity, especially TiO_2-HA with hollow structure, with T_{50} and T_{90} (temperature when 50% and 90% conversion were obtained) of approximately 175 °C and 201 °C, respectively (see Table 1). As referential samples, other three anatase, two brookite and one rutile TiO_2 catalysts were prepared through different methods, the XRD patterns and the DCM combustion activity of the samples are shown in Fig. S1 and the properties are shown in Table 1S. Also we can see that the same crystalline-phase TiO_2 catalysts prepared by different methods significantly differ in terms of activity (see Fig.S1). Furthermore, the synthesized catalyst was compared with catalysts recently reported in the literature, and the results are listed in Table 2. Notably, comparing the results of our work with those reported in the literature is difficult because the activity of the tested catalysts is significantly related to the operation condition. As listed in Table 2, the TiO_2-HA nanoparticle catalyst in the current work shows the highest

Table 2 some works made on total oxidation of DCM with catalyst

Catalyst	DCM Content / ppm	GHSV	T_{90}/℃	Ref.
Pt/Al_2O_3	1000	20000 h^{-1}	320	17
Ru/7%Ce-Al_2O_3	750	10000 h^{-1}	260	20
Ru/TiO_2	750	10000 h^{-1}	267	35
0.42k-2Pt/Al_2O_3	3000	15000 h^{-1}	321	7
Ce/TiO_2	1000	3000 h^{-1}	315	11
$CoCr_2O_4$	3000	15000 h^{-1}	257	13
4Ce1Cr	1000	9000 $mLg^{-1}h^{-1}$	337	10
$CuMnO_x$/Zr–Ti–Al	1200	8000 h^{-1}	470(T_{100})	36
H-ZSM-5	/	/	450(T_{100})	37
Mn/HZSM-5	1000	15000 h^{-1}	430	38
TiO_2-HA	1000	15000$mLg^{-1}h^{-1}$	201	This work

View Article Online
DOI: 10.1039/C6RA06400K

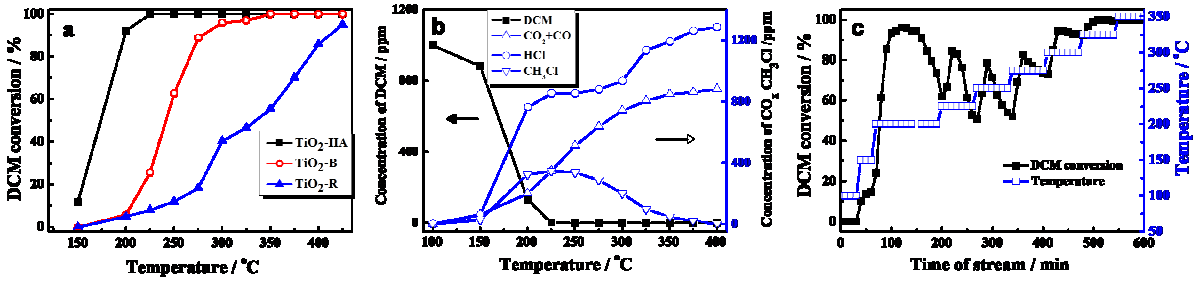

Fig. 2 Catalytic performance of DCM combustion on TiO_2-HA catalyst. (a) Light-off curves of DCM combustion on TiO_2-HA, brookite TiO_2 (TiO_2-B), rutile TiO_2 (TiO_2-R) ; (b) Catalytic Selectivity of DCM combustion on TiO_2-HA; (c) Stability of TiO_2-HA for DCM oxidation. Gas composition: 1000 ppm DCM in air, GHSV = 15000 mL h^{-1} $(gcat.)^{-1}$.

activity among all the employed catalysts, including noble metal catalysts, such as 0.42K-2Pt/Al_2O_3 and Ru/7%Ce-Al_2O_3, with T_{90} of 321 °C and 260 °C, respectively. It should be noticed that for CVOCs oxidation, high conversion is not only criterion for good catalyst systems, and selectivity of the products are also important. The desired products in Cl-containing CVOCs oxidation should be CO_2 and HCl. Fig.2b shows the conversion and products distribution of DCM over the TiO_2-HA catalyst. The detectable final products are CO_2, CO, and HCl with CH_3Cl. No other Cl-containing organic compounds are detected (see Fig. S3). Though TiO_2-HA have excellent catalytic activity at a low temperature range (below 225 °C), DCM conversion generated a large amount of CH_3Cl until reaching the plateau at 225 °C, indicating that the polar C-Cl bonds are much weaker than the C-H bonds and were expected to be cleaved at first.[39] It could be found that the yields of by-products decreased and a large amounts of (CO_2+CO) and HCl were generated with the temperature raising. In addition, HCl yield rapidly increased at 325 °C, which could be due to the sudden removal of many adsorbed Cl species in the form of HCl at this temperature. At 350 °C, most amount of DCM decomposed into simple (CO_2+CO) and HCl. The ratio of CO_2: (CO_2+CO) was about 29% at this temperature, hence, CO dominated in the generated (CO_2+CO) for TiO_2 catalyst, which indicates that the activity for CO oxidation of the catalyst is poor probably owing to the weak ability to dissociate O_2.[40]

The stability of the TiO_2-HA catalyst with time on stream was also investigated (see Fig.2c). Degradation experiments were conducted on the TiO_2–HA catalyst, which was maintained for 2 h at 200 °C. The DCM conversion was sustained at 90% during the first 90 min of the reaction, but it sharply decreased from 93% to 61% in the next 30 min. The conversion recovers when the temperature increases to 225 °C, but still decline later and even below 61%. Similar situation was observed at 250°C, 275°C and 300 °C. Until the temperature increase to 325 °C, the conversion only slightly declines in 1 h. At 350 °C, the DCM conversion maintains 100% in 1 h, we remain the temperature for another 50 h, and no significant deactivation is observed because the conversion still maintains above 90%. The deactivation of the catalyst at a low temperature which may be related to the Cl species deposited on the active sites in the process of DCM destruction on the surface of TiO_2-HA catalyst, and the increase of temperature can remove the adsorbed Cl species, hence, more active sites can be accessible.[20,35]Thus, at 350 °C for TiO_2-HA catalyst, the DCM removal activity remains without any catalyst deactivation on 50 h long-time stability tests, which suggests the presence of balance was found between absorbed Cl species and desorbed Cl species. And at this temperature, the DCM was transformed into HCl, (CO_2+CO) and hardly any CH_3Cl.

As previously mentioned, the activity for catalytic

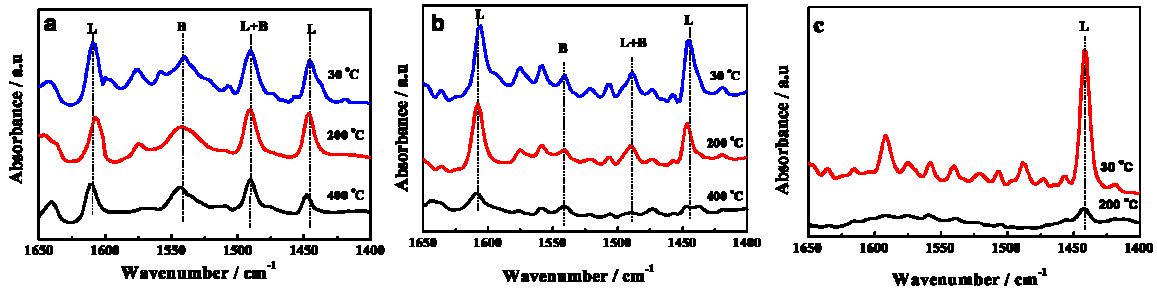

Fig. 3 Pyridine adsorption-temperature programmed desorption FT-IR for TiO_2. (a) TiO_2-HA, (b) brookite TiO_2 (TiO_2-B), (c) rutile TiO_2 (TiO_2-R).

View Article Online
DOI: 10.1039/C6RA06400K

combustion of DCM was considered related to the synergy between acidic role and oxidization. The acidity is favorable for activating C-Cl bonds. Thus, FTIR-pyridine was characterized the acidity on the catalysts surface (see Fig.3), measured after evacuation at 30°C, 200°C and 400 °C corresponding respectively to the amount of weak, mid-strong and strong acidity. The amount of Brønsted sites (B sites) and Lewis sites(L sites) was determined by the integration of the area of the peaks at 1537 and 1446 cm^{-1},[23,41] corresponding respectively to pyridine adsorbed on B sites and L sites. We find a very interesting phenomenon. In particular, the TiO_2-HA catalyst (see Fig.3a), possesses both B sites and L sites, and the increase in the evacuation temperature of pyridine induces a slight decrease in the peak of adsorbed pyridine on B acid sites and large decrease in L acid sites at 400°C.This phenomenon reveals that the B sites of the catalyst are mainly strong B sites and the L sites are mostly mid-strong L sites with a few strong L sites. In contrast, TiO_2-B and TiO_2-R exhibit no B sites; TiO_2-B possesses a certain amount of mid-strong L sites whereas the L sites of the TiO_2-R catalyst is mainly weak L sites (see Fig.3b-c). These observations indicate that the amount of mid-strong acid sites of the catalyst surface is corresponding with the catalytic activity. TiO_2-HA with strong B acid sites exhibits superior activity than TiO_2-B who has no B acid sites, which confirmed that the exposure of more B acid sites on the catalyst surface results in an enhancement of catalytic performances.[23]

Based on the above discussion and considerable literatures [5, 17, 42, 43], a plausible reaction mechanism for the catalytic combustion of DCM over TiO_2 catalyst was proposed. The first step was the reaction between a DCM molecule and one hydroxyl group that leads to the rupture of C–Cl bonds and freeing one HCl (or the Cl species adsorbed on the surface). The adsorbed intermediate species could be attacked by the adjacent activate oxygen species, the chlorine atom is substituted by oxygen atoms, leading to adsorbed formaldehyde formation and hemiacetal species, which disproportionate into methoxy species and formate species. The formaldehyde species could generate major methoxy species when this species accumulated a certain amount.[10 19]Giventhe weak redox property of TiO_2-HA, the intermediate formaldehyde species could not be immediately oxidized. Accordingly, amounts of CH_3Cl at low temperature were generated.

Notably, the interpretation of the superior activity of the TiO_2-HA catalyst remains in the preliminary stage. Subsequently, we will conduct several works to provide further explanation and basis for research on the modification of hollow TiO_2 surface to improve selectivity to CO_2 and ensure stability at low temperatures.

Hollow anatase TiO_2 nanoparticle is an excellent catalyst for DCM combustion, and shows the highest activity among all employed catalysts and exhibits a good selectivity to HCl and (CO_2+CO). The superior activity of the hollow TiO_2 catalyst could be attributed to its high surface area and larger amount of moderately strong acidic sites. This work may open a new direction of possibility for development of metal oxide catalysts for the catalytic combustion of industrial alkyl chlorides.

Acknowledgements

We would like to acknowledge the financial support from the Natural Science Foundation of China (NO. 21107096, 21506194), Zhejiang Provincial Natural Science Foundation of China (NO.Y14E080008, Y16B070025), the Commission of Science and Technology of Zhejiang province (NO. 2013C03021) and Specialized Research Fund for the Doctoral Program of Higher Education (NO. 20133317110004).

Notes and references

1 M. J. Morra, V. Borek, J. Koolpe.,*J. Environ. Qual.*, 2000, 29, 706.
2 J. J. Spivey, Ind. Eng. *Chem. Res*., 1987, 26, 2165.
3 J. N. Armor, *Appl. Catal., B*, 1992, 1, 221.
4 J. Hermia, S. Vigneron,*Catal. Today*., 1993, 17, 349.
5 X. Zhang, H. Lu, H. Huang, *RSC. Adv.*, 2015, 5, 79192.
6 Q. Dai, S Bai, X Wang, G Lu. *Appl. Catal., B*, 2013,129, 580.
7 Y. Wang, H Liu, S. Wang, M. Luo, J. Lu, *J. Catal.*, 2014, 311,314.
8 S. Pitkäaho, T. Nevanperä, L. Matejova, S. Ojala and R. L. Keiski, *Appl. Catal., B*, 2013, 138–139, 33.
9 S. Pitkäaho, L. Matejova, S. Ojala, J. Gaalova and R. L. Keiski, *Appl. Catal., B*, 2012, 113–114, 150.
10 P. Yang, S. Yang, Z. Shi, Z. Meng, R. Zhou. *Appl. Catal., B*, 2015, 162, 227.
11 S. Cao, H. Wang, F. Yu, M. Shi, S. Chen, X. Weng, Y. Liu, Z. Wu, *J. Colloid Interface Sci.*, 2016, 463, 233.
12 Q. Dai, L. Yin, S. Bai, W. Wang, X. Wang, X. Gong, G. Lu. *Appl. Catal., B*, 2016, 182, 598.
13 Y. Wang, A. Jia, M. Luo, J. Lu. *Appl. Catal., B*, 2015, 165, 477.
14 X. Wang, L. Ran, Y. Dai, Y. Lu, Q. Dai. *J. Colloid Interface Sci.*, 2014, 426, 324.
15 Y. Dai, X. Wang, Q. Dai, D. Li. *Appl. Catal., B*, 2012, 111-112, 141.
16 A. Aranzabal, M. Romero-S′aez, U. Elizundia, J. R. Gonz′alez-Velasco and J. A. Gonz′alez-Marcos, *J. Catal.*, 2012, 296,165.
17 I. Maupin, L. Pinard, J. Mijoin, P. Magnox. *J. Catal.*, 2012, 291, 104.
18 D. M. Papenmeier, J. A. Rossin, *Ind. Eng. Chem. Res*., 1994, 33, 3094.
19 R.W. van den Brink, P. Mulder, R. Louw, G. Sinquin, C. Petit, J.P. Hindermann, *J. Catal.*, 1998, 180, 153.
20 L Ran, Z. Wang, X. Wang, *Appl. Catal., A*, 2014, 470, 442.
21 R. López-Fonseca, B. de Rivas, J. I. Gutiérrez-Ortiz, A. Aranzabal, J. R. González-Velasco. *Appl. Catal., B*, 2003, 41, 31.
22 P. S. Chintawar, H. L. Greene, *Appl. Catal., B*, 1997, 13, 81.
23 F. Bertinchamps, C. G. Refoire, E. M. Gaigneaux, *Appl. Catal., B*, 2006, 66, 10.
24 R. López-Fonseca, A. Aranzabal, J. I. Gutierrez-Ortiz, *Appl. Catal., B*, 2001, 30(3-4), 303.
25 Q. Huang, X. Xue, R. Zhou, *J. Mol. Catal. , A*, 2010, 331(1-2), 130.
26 A. Aranzabal, J. A. Gonzalez-Marcos, P. Magnoux, et al, *Appl. Catal., B*, 2009, 88, 553.
27 H. Y. Huang, R. T. Yang, *Langmuir*, 2001, 17, 4997.
28 G. Busca, L. Lietti, G. Ramis, *Appl. Catal., B*, 1998, 18, 1.
29 J. P. Chen, R. T. Yang, *J. Catal.,* 1993, 139, 277.
30 M. Guo, L. Li, H. Lin, Y. Zuo, X. Huang and G. Li,*Chem. Commun.*, 2013, 49, 11752.
31 X. Shen, J. Zhang, B. Tian,*J. Hazard. Mater.*, 2011, 192, 651.
32 Q. Dai, X. Wang and G. Lu, *Appl. Catal., B*, 2008, 81, 192.
33 L. Y. Hsu, H. Teng, *Appl. Catal., B*, 2001, 42, 69.
34 X. S. Shang, G. R. Hu, C. H, J. P. Zhao, F. W. Zhang, *J. Ind. Eng. Chem.*, 2012, 18, 513.
35 L. Ran, Z. Qin, Z. Wang, X. Wang, Q. Dai, *Catal. Commun.*, 2013, 37, 5.
36 Y. Gu, Y. Yang, Y. Qiu, K. Sun, X. Xu, *Catal. Commun.*, 2010, 12, 277.
37 L. Intriago, E. Diaz, S. Ordonez, A. Vega, *Micropor. Mesopor. Mat.*, 2006, 91, 161.
38 J. I. Gutiérrez-Ortiz, R. López-Fonseca, U. Aurrekoetxea, J.R. González-Velasco, *J. Catal.*, 2003, 218, 148.
39 J. Haber, T. Machej, M. Derewinski, R. Janik, J. Krysciak, H. Sadowska, J. Janas, *Catal. Today.*, 1999, 54, 47.
40 M. A. G. Hevia, A. P. Amrute, T. Schmidt, J. Pérez-Ram, *J. Catal*., 2010, 276, 141.
41 C. A. Emeis, *J. Catal.*, 1993, 141, 347.

View Article Online
DOI: 10.1039/C6RA06400K

42 R. W, Van den Brink, R. Louw, P. Minder, *Appl. Catal., B*, 1998, 16, 219.
43 R. W, Van den Brink, M. Krzan, M. M. R. Feijen-Jeurissen, R. Louw, P. Minder, *Appl. Catal., B*, 2000, 24, 255.

View Article Online
DOI: 10.1039/C6RA06400K

Table of Content (TOC)

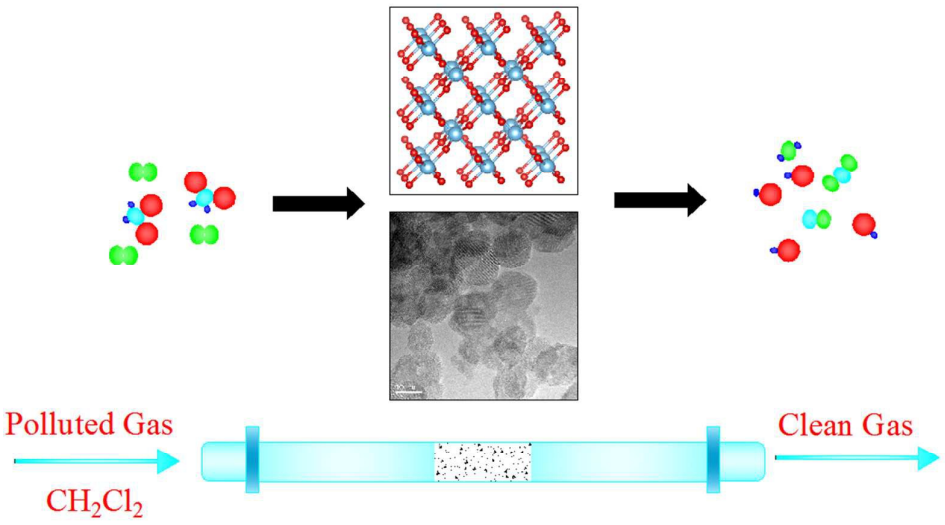

Hollow anatase TiO_2 nanoparticles with around 11.4 nm were prepared by CTAB-assisted hydrothermal method. This catalyst delivered a high catalytic activity for dichloromethane (DCM) combustion. In particular, the catalyst exhibited 90% DCM conversion at 201 °C.

Keywords

Hollow; Anatase TiO_2; DCM; Catalytic combustion;